

CRYSTAL GROWTH OF MATERIALS FOR  
ELECTRO-OPTIC MODULATORS

by

Fritz V. Wald, Richard O. Bell, Andrew A. Menna

Tyco Laboratories, Inc.  
Bear Hill  
Waltham, Massachusetts 02154

Contract No. F19628-70-C-0288

Project No. 5130

FINAL REPORT

15 June 1970 - 14 June 1971

July 1971

The views and conclusions contained in this document are those of the authors and should not be interpreted as necessarily representing the official policies, either expressed or implied, of the Advanced Research Projects Agency, or the U.S. Government.

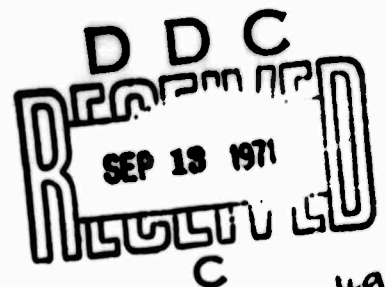
Approved for public release; distribution unlimited.

Contract Monitor: Charles S. Sahagian  
Solid State Sciences Laboratory

Sponsored by  
Advanced Research Projects Agency  
ARPA Order No. 1434

Monitored by  
AIR FORCE CAMBRIDGE RESEARCH LABORATORIES  
AIR FORCE SYSTEMS COMMAND  
UNITED STATES AIR FORCE  
BEDFORD, MASSACHUSETTS 01730

Reproduced by  
NATIONAL TECHNICAL  
INFORMATION SERVICE  
Springfield, Va. 22151



Unclassified

Security Classification

DOCUMENT CONTROL DATA - R & D

(Security classification of title, body of abstract and indexing annotation must be entered when the overall report is classified)

1. ORIGINATING ACTIVITY (Corporate author)  
Tyco Laboratories, Inc.

Bear Hill

Waltham, Massachusetts 02154

2a. REPORT SECURITY CLASSIFICATION

Unclassified

2b. GROUP

3. REPORT TITLE

CRYSTAL GROWTH OF MATERIALS FOR ELECTRO-OPTIC MODULATORS

4. DESCRIPTIVE NOTES (Type of report and inclusive dates)

Scientific. Final.

June 15, 1970 - June 14, 1971

Approved

18 August 1971

5. AUTHOR(S) (First name, middle initial, last name)

Fritz V. Wald

Richard O. Bell

Andrew A. Menna

6. REPORT DATE

July 1971

7a. TOTAL NO. OF PAGES

41

7b. NO. OF REFS

11

8a. CONTRACT OR GRANT NO.

F19628-70-C-0288

a. Project, Task, Work Unit Nos.

5130 n/a n/a

• DoD Element 61101F

DoD Subelement n/a

9a. ORIGINATOR'S REPORT NUMBER(S)

C008

9b. OTHER REPORT NO(S) (Any other numbers that may be assigned this report)

AFCRI.-71-0435

10. DISTRIBUTION STATEMENT

11. SUPPLEMENTARY NOTES

This research was supported by the Advanced Research Projects Agency.

Air Force Cambridge Research  
Laboratories (LQ)  
L.G. Hanscom Field  
Bedford, Massachusetts 01730

12. SUMMARY

This work covers two major topics. Firstly, crystal growth experiments on  $\alpha$ -HgS are reported. The aim here was to use the THM method of solution growth to grow large crystals from  $K_2S_4$  solvents. So far, no large crystals have been obtained but the general utility of  $K_2S_4$  as a solvent for the growth of smaller cinnabar crystals could be shown. Also, proustite, lead cesium chloride and bismuth sulfide were grown using the THM method.

Secondly, a method for the calculation of electrooptic coefficients of materials using only basic parameters was developed. Phillips electronegativities, crystallographic data and electronic polarizabilities of the atoms are used as inputs in a computer program which is described. The program outputs the electrooptic coefficients of cubic and noncubic structures. The major test cases were compounds of the zinc-blende structure and extremely good agreement between calculated and experimentally determined electrooptic coefficients is obtained.

DD FORM 1473

USE PREVIOUS EDITIONS, 1 JAN 64, WHICH IS OBSOLETE FOR ARMY USE.

Unclassified

Security Classification

Unclassified

Security Classification

14. KEY WORDS	LINK A		LINK B		LINK C	
	ROLE	WT	ROLE	WT	ROLE	WT
Electrooptic materials Cinnabar-HgS Proustite Crystal growth Electrooptic coefficient-theory						

Unclassified

Security Classification

MISSING PAGE  
NUMBERS ARE BLANK  
AND WERE NOT  
FILMED

ACCESSION NO.	
WFOI	WHITE SECTION <input checked="" type="checkbox"/>
DOO	DIFF SECTION <input type="checkbox"/>
UNANNOUNCED	<input type="checkbox"/>
JUSTIFICATION	
BY	
DISTRIBUTION/AVAILABILITY CODES	
OUT.	AVAIL. and/or SPECIAL
A	

Program Code No.	OD10
Effective Date of Contract	15 June 1970
Contract Expiration Date	15 June 1971
Principal Investigator and Phone No.	Fritz Wald 899-2400, Ext. 349
Project Scientist or Engineer and Phone No.	Charles S. Sahagian, 617 861- 3298

"Qualified requestors may obtain additional copies from the Defense Documentation Center. All others should apply to the National Technical Information Service."

**AFCRL-71-0435**

**CRYSTAL GROWTH OF MATERIALS FOR  
ELECTRO-OPTIC MODULATORS**

**by**

**Fritz V. Wald, Richard O. Bell, Andrew A. Menna**

**Tyco Laboratories, Inc.  
Bear Hill  
Waltham, Massachusetts 02154**

**Contract No. F19628-70-C-0288  
Project No. 5130**

**FINAL REPORT**

**15 June 1970 - 14 June 1971**

**July 1971**

**The views and conclusions contained in this document are those of the authors and should not be interpreted as necessarily representing the official policies, either expressed or implied, of the Advanced Research Projects Agency or the U.S. Government.**

**Approved for public release; distribution unlimited.**

**Contract Monitor: Charles S. Sahagian  
Solid State Sciences Laboratory**

**Sponsored by  
Advanced Research Projects Agency  
ARPA Order No. 1434**

**Monitored by  
AIR FORCE CAMBRIDGE RESEARCH LABORATORIES  
AIR FORCE SYSTEMS COMMAND  
UNITED STATES AIR FORCE  
BEDFORD, MASSACHUSETTS 01730**

### ABSTRACT

This work covers two major topics. Firstly, crystal growth experiments on  $\alpha$ -HgS are reported. The aim here was to use the THM method of solution growth to grow large crystals from  $K_2S_4$  solvents. So far, no large crystals have been obtained but the general utility of  $K_2S_4$  as a solvent for the growth of smaller cinnabar crystals could be shown. Also, proustite, lead cesium chloride and bismuth sulfide were grown using the THM method.

Secondly, a method for the calculation of electrooptic coefficients of materials using only basic parameters was developed. Phillips electronegativities, crystallographic data and electronic polarizabilities of the atoms are used as inputs in a computer program which is described. The program outputs the electrooptic coefficients of cubic and noncubic structures. The major test cases were compounds of the zinc-blende structure and extremely good agreement between calculated and experimentally determined electrooptic coefficients is obtained.

## Table of Contents

Section		Page No.
	ABSTRACT .....	iii
I.	INTRODUCTION.....	1
II.	WORK IN THE FIRST SIX MONTHS OF THE CONTRACT.....	3
III.	WORK IN THE FINAL SIX MONTHS OF THE CONTRACT.....	5
	A. Theory .....	5
	B. Crystal Growth .....	26
IV.	CONCLUSIONS.....	39
V.	REFERENCES .....	41

## List of Illustrations

Figure		Page No.
1	Schematic Representation of Solution Growth Process Using Simplifying Assumptions .....	15
2	Consequences of Using an Asymmetrical Temperature Distribution in the Solvent as in the THM Method.....	17
3	Temperature and Concentration in the Solvent Zone for the Equilibrium Case (Pure Diffusion).....	19
4	Relation of Liquidus Temperature and Actual Temperature for the Case of Pure Diffusion in THM .....	19
5	Relation of Concentration and Temperature for the Case of a Fully Stirred Liquid.....	20
6	Temperature and Concentration Distribution for the Case of a Partially Stirred Liquid.....	20
7	Effect of Temperature Fluctuations on the Concentration in a THM System.....	22
8	Change of Temperature Profile in the Solvent Zone for the Case of a Sudden Temperature Drop.....	22
9	Heat Flow and Isotherms in THM for the Case of Equal Thermal Conductivity in the Solid and the Liquid.....	23
10	Heat Flow and Isotherms in a Partially Mixed Liquid .....	25
11	Design of Present THM Furnaces.....	28
12	Typical Temperature Profile in a THM Furnace as Shown in Fig. 11.....	29
13	Cinnabar, Regrown from $K_2S_4$ in a THM Experiment.....	30
14	Schematic of $\alpha$ -HgS Vapor Growth Furnace.....	35
15	Longitudinal Section Through Vapor Grown Polycrystalline $\alpha$ -HgS Boule .....	36
16	Top of Vapor Grown $\alpha$ -HgS Ingot Showing a Series of Rods .....	36
17	Autoclave Used in Hydrothermal Growth Experiments .....	37

## I. INTRODUCTION

Recently it could be shown, in a number of instances, that certain methods of solution growth are capable of growing materials of interest for electrooptics which are otherwise difficult to prepare. The methods of solution growth used are the "Traveling Solvent Method" (TSM) and the "Traveling Heater Method" (THM), the latter one particularly applicable to the growth of larger crystals. Thus, growth of ZnO,<sup>1</sup>  $(\text{Pb}_x\text{Sr}_{1-x})\text{TiO}_3$ ,<sup>2</sup> and CdTe<sup>3</sup> was accomplished and for the latter two cases electrooptic modulation properties were demonstrated.

Since solution growth methods are often very powerful for the preparation of complicated compounds, in particular if solid state transformations, high vapor pressure, and deviations from stoichiometry are involved, it seems reasonable to test THM in particular as a method for growth of various complex sulfides and other compounds which are of interest as potentially useful modulator materials. In particular, the growth of sizable crystals of cinnabar ( $\alpha$ -HgS) has always presented some problems because of its phase transformation at 344 °C into metacinnabar, the cubic form. Thus, growth of  $\alpha$ -HgS crystals with sizes sufficient for electrooptic usage was the main objective of the program.

Although in some cases a unique necessity for crystal growth from solution exists, this is generally not the case. Alternative methods of single crystal preparation often exist. Nevertheless growth from solution, if properly conducted such as in the THM arrangement, leads often to far higher perfection and purity in the final crystal. This is due to the fact that: (1) growth occurs slowly under near equilibrium conditions, and (2) impurity segregation is often facilitated if a solvent is used.

Apart from these experimental objectives, a major theoretical objective has been adopted. This concerns the absence of reliable models for the calculation of various electrooptic properties of materials. Thus, work on a simple model,

based on readily accessible information of a physiochemical and crystallographic nature, which allows reliable calculation of electrooptic coefficients and other optical properties of crystalline materials has been carried out.

## II. WORK IN THE FIRST SIX MONTHS OF THE CONTRACT

This work is described in detail in Semianual Report No. 1 on the present contract, which was issued in January 1971 and will only be summarized here.

The major amount of experimental work in the first half of the contract was directed towards finding a suitable solvent for the THM growth of cinnabar. In the course of these experiments, a compound  $\text{Hg}_3\text{S}_2\text{I}_2$  was found and the phase diagram of the  $\text{HgS-HgI}_2$  system was delineated.

Nevertheless, the only suitable solvents found for  $\alpha$ - $\text{HgS}$  were polysulfides of sodium and potassium and initial growth experiments using these solvents were carried out without too much success.

Also  $\text{PbCsCl}_3$  was grown from  $\text{PbCl}_2$  melts. Although no single crystals resulted, the regrowth of polycrystalline boules clearly demonstrated that further cultivation of the method using a  $\text{PbCl}_2$  solvent would undoubtedly lead to the growth of large crystals. Since, however, the material does not seem to be of too much interest at present, further experimentation was discontinued.

Also, several experiments on the growth of proustite from  $\text{As}_2\text{S}_3$  rich solutions were undertaken. These experiments were quite successful in producing sizable clear crystals in several instances. There were indications from optical transmission measurements that through the use of an  $\text{As}_2\text{S}_3$  rich solvent the absorption peak around  $10\ \mu$  might be minimized or avoided. The disappearance of that absorption was not reproducibly observed in all samples grown, but one might be led to the conclusion that it could be caused by a native defect.

Further work in the first 6-month period of the contract was concerned with a literature search which covered  $\alpha$ - $\text{HgS}$ , proustite, lead-cesium chloride, and other ternary noncentrosymmetric compounds which might be of interest in electrooptics.

Finally, a major amount of work was devoted to the development of a theory which allows calculation of the electrooptic coefficients from basic parameters. The method uses as basic information only crystal structure data, lattice polarizabilities

and electronegativity differences. Computing the electrooptic coefficients for the cubic zincblende structure, very good agreement between the computed values and measured values was indeed obtained. Extension of the method to noncubic structures was also started and is described in detail in the body of this report.

and  $t_{ij}$  and  $s_{ij}$  are appropriately defined lattice sums. This expression has been derived for a rigid but polarizable ionic model under the assumption that the internal and external fields are parallel which is true for cubic materials or special cases in other symmetries. For example, in a hexagonal crystal, when the applied electric field is parallel to the c-axis or in the basal plane, the internal field will be in the same direction. An isotropic dielectric constant has been tacitly assumed.

In the more general case, an expression for the internal fields at the lattice sites has been derived. Without going into details, it can be shown that:

$$\begin{aligned} \vec{E}_i = & \frac{1}{3} (\epsilon + 2) \vec{E} + \sum_{j, n, m, l} \left\{ \frac{X_j}{4\pi} \frac{1}{|r_{ij}|^3} \left[ \vec{P}_j r_{ij}^2 \right. \right. \\ & - 3 (\vec{r}_{ij} \cdot \vec{P}_j) \vec{r}_{ij} \left. \right] + \frac{3}{2} \frac{(X_j + X_j'') X_j' \epsilon_0 v}{e_j |r_{ij}|^7} \left[ \left[ 5 (\vec{r}_{ij} \cdot \vec{P}_j)^2 \right. \right. \\ & \left. \left. - r_{ij}^2 P_j^2 \right] \vec{r}_{ij} - 2 (\vec{r}_{ij} \cdot \vec{P}_j) r_{ij}^2 \vec{P}_j \right] \right\} \end{aligned} \quad (4)$$

No simple general expression for the dielectric constant such as Eq. (1) can be written down. Note that here the dielectric constant is treated as a tensor and  $X_j'$  probably should, but has not.

Returning to the more restricted case, the first term on the right hand side in Eq. (2) for  $\epsilon_{ij}$  is the contribution to the dielectric constant by the polarizability of the ions. For optical frequencies where  $\epsilon = n^2$ , the ionic part of  $X_j$  will disappear (i.e.,  $X_j' = 0$ ). The second term is the Lorentz correction which can contribute to the dielectric constant if the structure of the lattice allows a large value for  $t_{ij}$  which occurs for ferroelectric materials such as  $\text{BaTiO}_3$ . The third term produces an electric field dependence of the dielectric constant or at optical frequencies gives rise to a linear electrooptic effect. This term vanishes for centrosymmetric materials. The next higher order term (which has not been written out) can produce the dielectric constant nonlinearity<sup>5</sup> and quadratic electrooptic effect observed in materials such as  $\text{SrTiO}_3$ .<sup>6</sup>

Let us now consider the specific case of the wurtzite structure. Table I shows the location of the four atoms in the hexagonal unit cell. Also shown are the vectors,

**Table 1. Coordinates of Atoms and Lattice Vectors  
in the Wurtzite Hexagonal Unit Cell - AB**

**Coordinates of Atoms**

Atomic Position	x	y	z
A-atoms 1	ma	na	lc
2	$(m + \frac{1}{3}) a$	$(n + \frac{2}{3}) a$	$(l + \frac{1}{2}) c$
B-atoms 3	ma	na	$(l + u) c$
4	$(m + \frac{1}{3}) a$	$(n + \frac{2}{3}) a$	$(l + \frac{1}{2} + u) c$

**Coordinates of Lattice Vector**

Lattice Vectors	x	y	z
$r_{11} = r_{22} = r_{33} = r_{44}$	ma	na	lc
$r_{12} = r_{34}$	$(m + \frac{1}{3}) a$	$(n - \frac{1}{3}) a$	$(l + \frac{1}{2}) c$
$r_{13} = r_{24}$	ma	na	$(l + u) c$
$r_{14}$	$(m + \frac{1}{3}) a$	$(n - \frac{1}{3}) a$	$(l + u - \frac{1}{2}) c$
$r_{23}$	$(m - \frac{1}{3}) a$	$(n + \frac{1}{3}) a$	$(l + u - \frac{1}{2}) c$

In an ideal wurtzite lattice,  $c/a = \sqrt{8/3}$  and  $u = 3/8$ .

$\hat{r}_{ij}$ , that connect the different lattice sites. Table II shows the lattice sites for cinnabar using the three molecule unit cell. (Nothing further has been done with calculations on cinnabar this report period, and we will restrict ourselves to wurtzite.)

Writing out Eq. (1):

$$\frac{\epsilon - 1}{\epsilon + 2} = \frac{1}{3} \left\{ 2(X_A + X_B) + (2t_{11} + 2t_{12} + 2t_{13} + t_{14} + t_{23})(X_A^2 + X_B^2) + (2s_{11} + 2s_{12} + 2s_{13} + s_{14} + s_{22})[\beta_A(X_A + X_A'') + \beta_B(X_B + X_B'')] \right\} \quad (5)$$

where

$$t_{ij} = \frac{v}{4\pi} \sum_{n, m, l} \frac{r_{ij}^2 - 3(\hat{n} \cdot \hat{r}_{ij})}{|r_{ij}|^7} \quad (6)$$

$$s_{ij} = \frac{v}{8\pi} \sum_{n, m, l} \frac{3(\hat{n} \cdot \hat{r}_{ij})[5(\hat{n} \cdot \hat{r}_{ij})^2 - 3r_{ij}^2]}{|r_{ij}|^7} \quad (7)$$

where  $\hat{n}$  is either along the  $z$  (optic) axis or in the basal plane. Use has been made of the symmetry of  $t_{ij}$  and  $s_{ij}$  to reduce the number of independent components. The solution for an arbitrary direction is not obvious as Eq. (4) would have to be used. Also the anisotropy of  $\epsilon$  has been neglected.

We will choose as the coordinate system that of the axes of the hexagonal unit cell which is nonorthogonal. Thus:

$$\hat{r}^2 = x^2 + y^2 - xy + z^2$$

if  $x$ ,  $y$ , and  $z$  are the three components of  $\hat{r}$ .

Also:

$$\hat{r} \cdot \hat{n} = xn_1 + yn_2 - \frac{1}{2}(xn_2 + yn_1) + zn_3$$

where  $n_1$ ,  $n_2$ , and  $n_3$  are the three components of  $\hat{n}$ .

**Table II. Coordinates of Atoms in Cinnabar Using A Trimolecular Hexagonal Unit Cell**

Atomic Position		Coordinates of Atoms		
		x	y	z
Hg-atoms	1	$(m + u) a$	n	$(l + \frac{1}{3}) c$
	2	ma	$(n + u) a$	$(l + \frac{2}{3}) c$
	3	$(m - u) a$	$(n - u) a$	lc
S-atoms	4	$(m + v) a$	na	$(l + \frac{5}{6}) c$
	5	ma	$(n + v) a$	$(l + \frac{1}{6}) c$
	6	$(m - v) a$	$(n - v) a$	$(l + \frac{1}{2}) c$

$$u = 0.720$$

$$a = 4.149$$

$$v = 0.495$$

$$c = 9.495$$

The computer program to perform these sums is shown below.

Generally the calculations of lattice sums can be performed in a straightforward manner. Using a computer, the calculations are made over successively larger and larger volumes about the origin which allows using a Neville plot to extrapolation to infinite volumes. A Neville plot is plot of the sum versus  $N^{-1}$  where  $N$  is the total number of atoms over which the sum is performed, thus extrapolating to where  $N^{-1}$  is zero gives the limit of the sum.<sup>7</sup> This approach is particularly effective when the terms have the form of  $r^{-n}$  where  $n > 3$ . If  $n \leq 3$ , convergence can be a problem unless some care is taken to arrange the terms so that contributions from negative and positive terms nearly cancel. In this program the use of a spherical volume worked fairly well. This was checked since it is known that  $(2t_{11} + 2t_{12} + 2t_{13} + t_{14} + t_{23})$  should be zero for wurtzite, and when the calculation was made this quantity was small.

The first part of the program inputs the value of  $c/a$ ,  $u$ , and the largest value of  $r$  over which the sum is to be made. The four separate sums are calculated at the same time and are identified such that the index 1 corresponds to 11, 2 to 12, 3 to 13, and 4 to 14. The sum is then made over each atom by calling the subroutine appropriate to the external electric field being applied parallel or perpendicular to the  $c$ -axis. Typical output is shown where the sum is shown for each term over larger unit cells. In this particular case for an electric field along the  $c$ -axis,  $s_{12}$  and  $s_{11}$  are zero. Eq. (1) or (5) can be used to calculate the change in dielectric constant or electrooptic effect since  $n^2 = \epsilon$  and  $X_j^i = 0$ .

## 2. Computer program for lattice sums

The following program was used to calculate the lattice sums.

```

C PROGRAM TO CALCULATE LATTICE SUMS FOR A WURTZITE STRUCTURE
      DIMENSION A(5),C(5),G(5)
      COMMON COA,XY2,NION5
      TYPE 13
      13 FORMAT (///' INPUT U, C/A, MAX: ( )'
      ACCEPT 22, U,COA,MAX
      22 FORMAT(3F10.3)
      C COA IS THE RATIO OF C/A ABOUT 1.633.
      C MAX IS THE FURTHEST ION OVER WHICH THE SUM IS TO BE MADE.
      C U IS A STRUCTURE PARAMETER APPROXIMATELY EQUAL TO 0.175.
      PAGE=COA*SQRT(3.)/C./3.141592

```

A, B, AND C ARE THE COORDINATES OF ATOMS IN THE PRIMITIVE CELL.

```

A(1)=0.
A(2)=1./3.
A(3)=0.
A(4)=A(2)
B(1)=0.
B(2)=-A(2)
B(3)=0.
B(4)=B(2)
C(1)=0.
C(2)=.5
C(3)=0
C(4)=0-.5
V=0
TYPE 30, FAC, 1, COA, MAX, K
30 FORMAT(3F10.6, 2I5 //)
TYPE 35
35 FORMAT(// '      TERM      TT      SS      A      B
1      C      IONG      ')
70 K=K+1
KK=2*K+1
TTT=0.
KK2=K**2
DO 50 J=1, 4
TT=0.
SS=0.
NIONC=0
AA=A(I)
BB=B(I)
CC=C(I)
DO 40 NN=1, KK
XN=NN-1-K
DO 40 MM=1, KK
XM=MM-1-K
DO 40 LL=1, KK
XL=LL-1-K
C THE CONTRIBUTION IS CALCULATED FOR EACH TERM WITHIN A
C SPHERE OF RADIUS V.
CALL TERM(XN, XM, XL, AA, BB, CC, T, C)
TT=TT+T
SS=SS+C
40 CONTINUE
TT=TT+FAC
SS=SS+FAC/2.
TTT=TTT+TT
50 TYPE 30, J, TT, SS, AA, BB, CC, NIONC
60 FORMAT(3X, I3, 2F14.5, 3F8.4, I5 )
TYPE 30, TTT
80 FORMAT(//, 5X, 'THE SUM OF TT IS ', F14.5 )
TYPE 65
65 FORMAT (/)
IF(V.LT. MAX) GO TO 70
CONTINUE
END.

```

The subroutine for the case the electric field is along the c-axis is the following:

```

C CALCULATION OF TERMS IN THE SUM FOR C-AXIS WURZITE.
SUBROUTINE TERM(X,Y,Z,A,P,C,T,C)
COMMON CA,XY2,N
S=0.
T=0.
IF(X*X+Y*Y+Z*Z*CA*CA-X*Y.GT.XK2)RETURN
RDR=(X+A)*(X+A)+(Y+P)*(Y+P)-(X+A)*(Y+P)+(Z+C)*(Z+C)*CA*CA
IF(RDR.EQ.0.) RETURN
N=N+1
RDN=(Z+C)*CA
T=(RDR-3.*RDN*RDN)/RDR**2.5
C=3.*RDN*(5.*RDN+RDN-3.*RDR)/RDR**3.5
RETURN
END

```

Typical output is shown below:

INPUT U, C/A, MAX: .375 1.6329931 6

0.112540 0.375000 1.632993 6 0

TERM	TT	SS	A	P	C	IONS
1	0.67524E+00	0.00000E+00	0.0000	0.0000	0.0000	6
2	-0.32318E+00	0.39455E-01	0.3333	-0.3333	0.5000	7
3	-0.90400E+00	0.10430E+01	0.0000	0.0000	0.3750	7
4	0.11653E+01	0.32460E+01	0.3333	-0.3333	-0.1250	7
SUM OF TT IS		0.61337E+00				
1	0.55892E+00	0.00000E+00	0.0000	0.0000	0.0000	32
2	-0.64500E+00	-0.10149E+00	0.3333	-0.3333	0.5000	33
3	-0.11903E+01	0.10405E+01	0.0000	0.0000	0.3750	33
4	0.11106E+01	0.31891E+01	0.3333	-0.3333	-0.1250	33
SUM OF TT IS		-0.17574E+00				

1	0.59991E+00	0.00000E+00	0.0000	0.0000	0.0000	74
2	-0.55657E+00	-0.42276E-02	0.3333	-0.3333	0.5000	75
3	-0.11228E+01	0.17002E+01	0.0000	0.0000	0.3750	75
4	0.11402E+01	0.31761E+01	0.3333	-0.3333	-0.1250	75

SUM OF TT IS 0.60769E-01

1	0.57765E+00	-0.13101E-09	0.0000	0.0000	0.0000	200
2	-0.57493E+00	-0.49174E-02	0.3333	-0.3333	0.5000	200
3	-0.11453E+01	0.16972E+01	0.0000	0.0000	0.3750	200
4	0.11174E+01	0.31731E+01	0.3333	-0.3333	-0.1250	200

SUM OF TT IS -0.25107E-01

1	0.57861E+00	-0.25875E-09	0.0000	0.0000	0.0000	384
2	-0.57079E+00	0.88484E-03	0.3333	-0.3333	0.5000	385
3	-0.11417E+01	0.17017E+01	0.0000	0.0000	0.3750	385
4	0.11176E+01	0.31719E+01	0.3333	-0.3333	-0.1250	385

SUM OF TT IS -0.16303E-01

1	0.56997E+00	0.19816E-09	0.0000	0.0000	0.0000	636
2	-0.58012E+00	-0.20511E-03	0.3333	-0.3333	0.5000	637
3	-0.11503E+01	0.17009E+01	0.0000	0.0000	0.3750	637
4	0.11001E+01	0.31722E+01	-0.3333	-0.3333	-0.1250	637

SUM OF TT IS -0.51999E-01

### **3. Crystal growth by THM: A detailed qualitative process analysis\***

---

Any analysis of THM must consider the fact that the diffusion process is convection aided, as well as external experimental variables such as heat flow through solvent and the adjacent solids, etc.

Recently, such an initial qualitative analysis was carried out by Tyco personnel working under several contracts which use the THM method (including the one on which we report) with the help of Professor Bruce Chalmers of Harvard University, who is a consultant to Tyco on crystal growth matters. The results of this initial analysis are reported in this section.

Essentially what is being done is to analyze the conditions for steady state THM growth under various experimental constraints. Without serious loss of precision, the following assumptions are made:

1. The relevant liquidus line is straight.
2. The solidus line is vertical.
3. Each solid-liquid interface is at the liquidus temperature for the liquid at the interface. (This implies that growth is slow enough for kinetic supercooling to be neglected.)

The following sequence is adopted:

1. Description of the process
2. Solute and temperature distribution in the liquid zone: (a) when transport is by diffusion alone, (b) when stirring is completely effective, and (c) when stirring is partially effective
3. Effect of temperature fluctuations
4. The shape of the interface.

#### **The Process**

For the present purpose, the process can be represented by Fig. 1 in which a liquid zone moves upwards relative to the growing crystal C. The relevant part of the phase diagram is shown in the right hand part of the figure. The liquid

---

\*F. Wald.

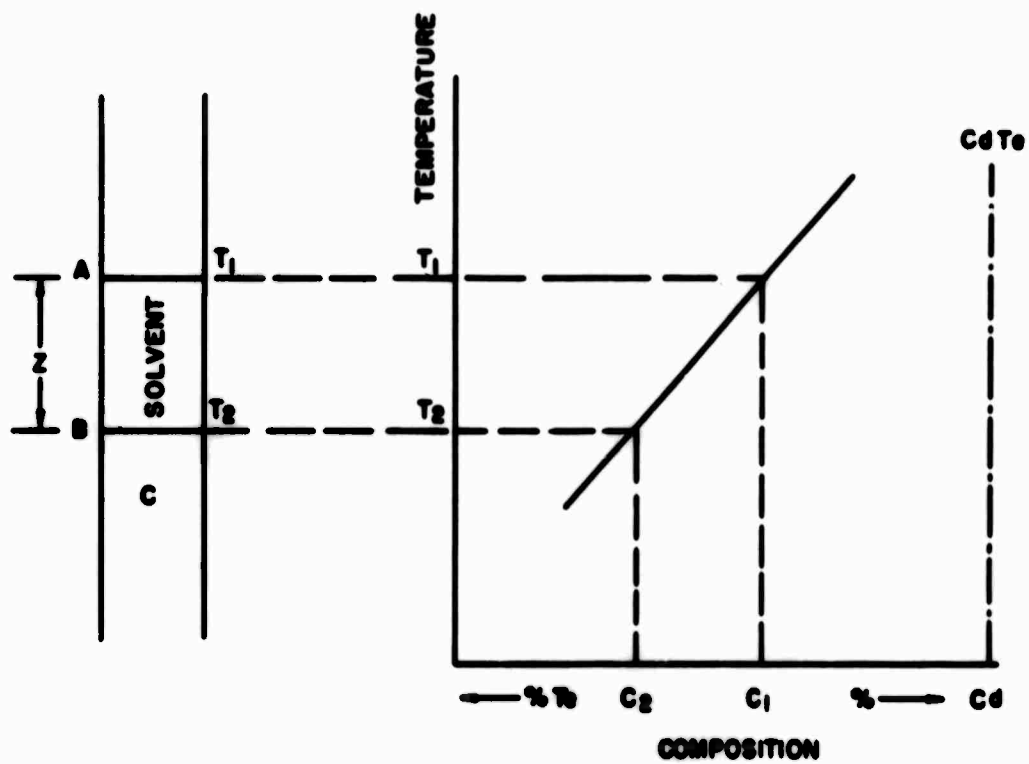


**Fig. 1. Schematic representation of solution growth process using simplifying assumptions**

zone AB has a thickness  $Z$ , which is essentially independent of temperature and speed. The liquid at A has a composition  $C_1$ , and that at B,  $C_2$ . There is, therefore, a concentration gradient of average value  $(C_1 - C_2)/Z$  through which transport takes place, tending to increase the concentration at B and to reduce it at A. This tendency is prevented by crystal growth at B and solution at A. The process will continue so long as  $T_1 > T_2$ . This temperature difference can be maintained in two ways: (1) by imposing a temperature gradient on the system, and moving the temperature profile relative to the sample at an appropriate rate, or (2) by supplying heat assymetrically to the liquid zone by continuous relative motion and extracting it from the two solid regions. The heat source is moved relative to the sample. (This latter is truly the essence of the THM process.)

It can be shown that the second method (heated zone) offers much more flexibility than the first (moving gradient). Assuming (for the moment) that transport is purely by diffusion, the following conditions would exist. With a fixed temperature gradient [Case (1)] and a fixed zone length,  $T_1 - T_2$ ,  $C_1 - C_2$  and  $Z$  would be fixed; this would produce a flux  $[D(C_1 - C_2)/Z]$  through the zone, which would define the rate of growth. Unless the temperature gradient is moved at the same speed, the solvent zone would move continuously up or down the temperature gradient, and no steady state would be possible. In the second case, on the other hand (Fig. 2.), a fixed zone length would be compatible with a wide range of temperature differences (from zero to  $T_3 - T_4$  in Fig. 2), and a correspondingly wide range of values of  $C_1 - C_2$ . The flux through the zone can, therefore, adjust itself, by suitable positioning of the zone, to cause crystal growth at any speed within a wide range. There is, therefore, considerable latitude in the speed at which continuous steady state growth can occur for a given temperature profile. This will change only in detail but not in significance if the difference in thermal conductivities between the solvent and the solid is to be taken into account.

#### Solute and Temperature Distribution in the Liquid Zone

Three types of defects may occur: (1) "stray" crystals, (2) inclusions, and (3) cellular substructures. These can all arise from either general or local supercooling of the liquid near the growth interface. General supercooling is that which occurs right across the section, as opposed to local, which does not. Since heat is applied to the liquid, the latter must (if we assume a planar interface) be at

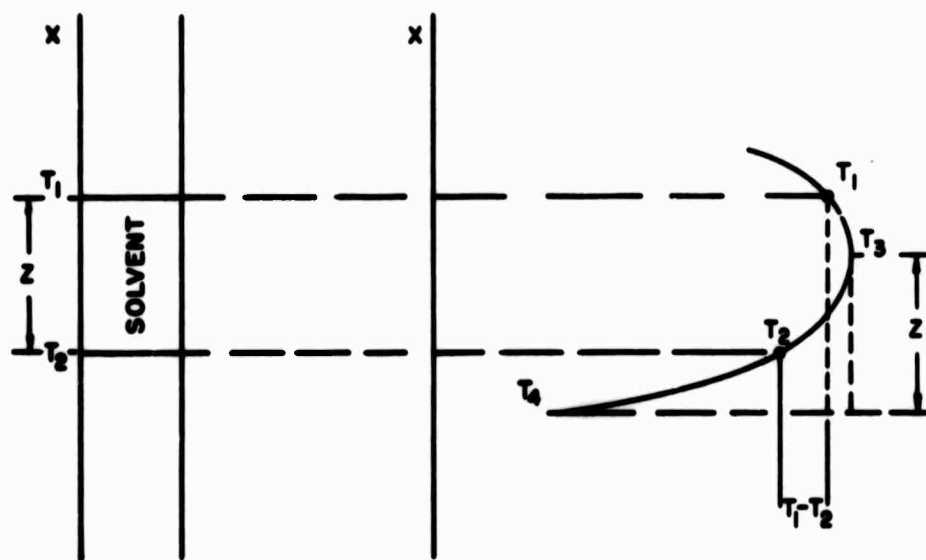


**Fig. 2.** Consequences of using an asymmetrical temperature distribution in the solvent as in the THM method

a higher temperature than  $T_2$ ; the only supercooling that can occur, therefore, would be constitutional. We will consider the relationship between composition and temperature for a planar interface, making various assumptions about the mechanism of transport. Three assumptions will be made: (a) transport by diffusion alone (no mixing,) (b) completely effective mixing, (c) complete mixing except for a stagnant diffusion zone at each end.

a. Diffusion alone: Steady state diffusion from interface I to interface II requires a uniform gradient of composition. If the temperature difference is maintained by a uniform temperature gradient (Fig. 3), the temperature of the liquid would be equal to its liquidus at all points. If the heat is supplied to the liquid, the distribution of temperatures [actual ( $T_a$ ) and liquidus ( $T_L$ )] is shown in Fig. 4. The actual temperature is everywhere above the liquidus, and there is no supercooling.

b. Complete mixing: This would give a composition profile as shown in Fig. 5. The liquidus temperature would be as shown in the center portion of the figure which also shows a uniform gradient (unrealistic in a fully mixed liquid) and a temperature profile  $T_A$  that might exist in a stirred heated liquid. In the latter case, there is a small supercooled zone.

c. Partial mixing: The temperature distribution for the heated liquid case would be as shown (Fig. 6), the stagnant zones having high temperature gradients. There could be a small supercooled zone, but the fact that the "mixed region" applied to temperature as well as to solute suggests that a substantial region of supercooling is not to be anticipated.

The general conclusion of this section is that under realistic experimental conditions and assuming a planar interface, there is no severe constitutional supercooling in THM.

#### Effect of Temperature Fluctuations

We will consider the possible effect of temperature fluctuations that take place too fast for diffusion to occur over distances comparable with the thickness of the liquid zone (if  $Z = 1$  cm,  $D = 10^{-5}$  cm<sup>2</sup>/sec; then, since  $d^2 = \nabla T$ ,  $t = 10^5$  sec). Therefore, fluctuation of period, say 1 minute or 1 hour would qualify; but a period of 1 day would not. Assume that steady state has been achieved ("diffusion only" case); the liquid at I is at  $C_1$ , etc. (Fig. 7). Now lower the temperature to  $T_1'$

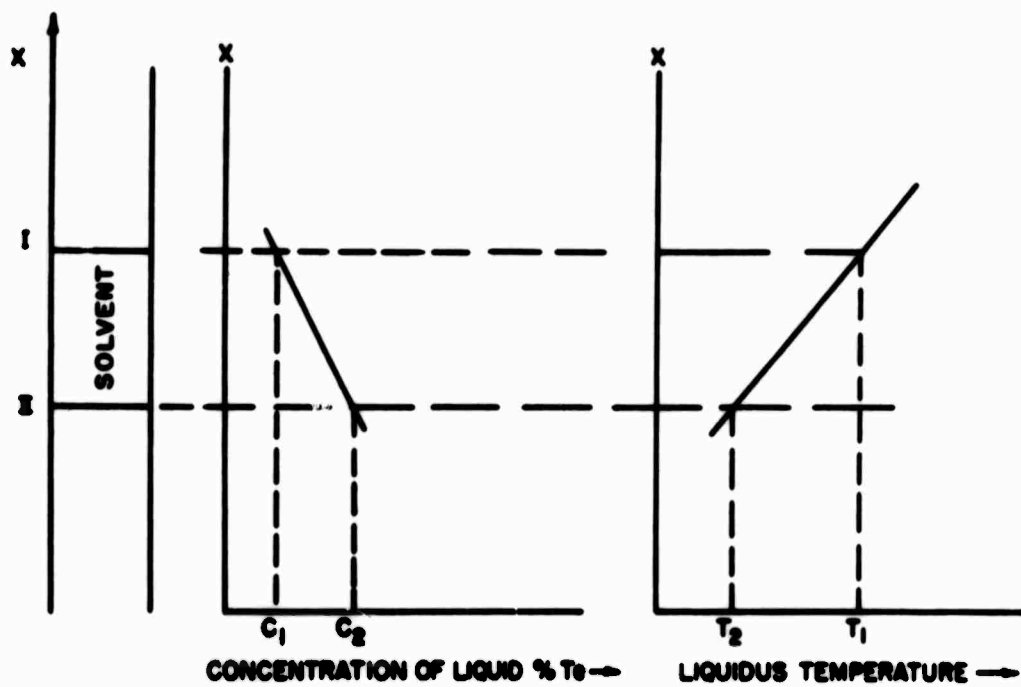


**Fig. 3.** Temperature and concentration in the solvent zone for the equilibrium case (pure diffusion)

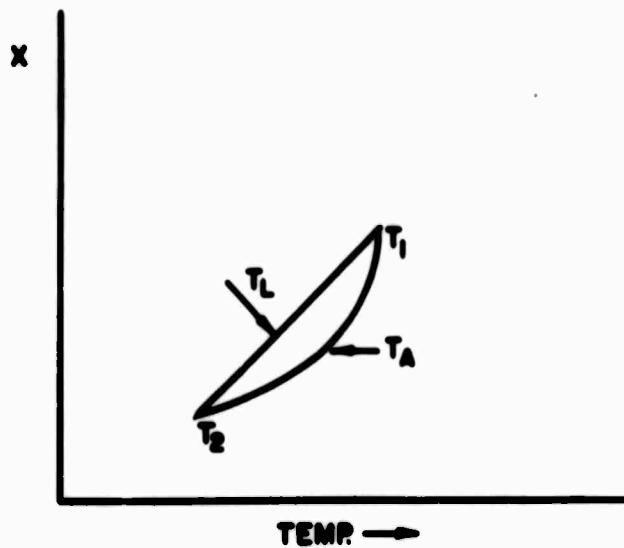


**Fig. 4.** Relation of liquidus temperature and actual temperature for the case of pure diffusion in THM

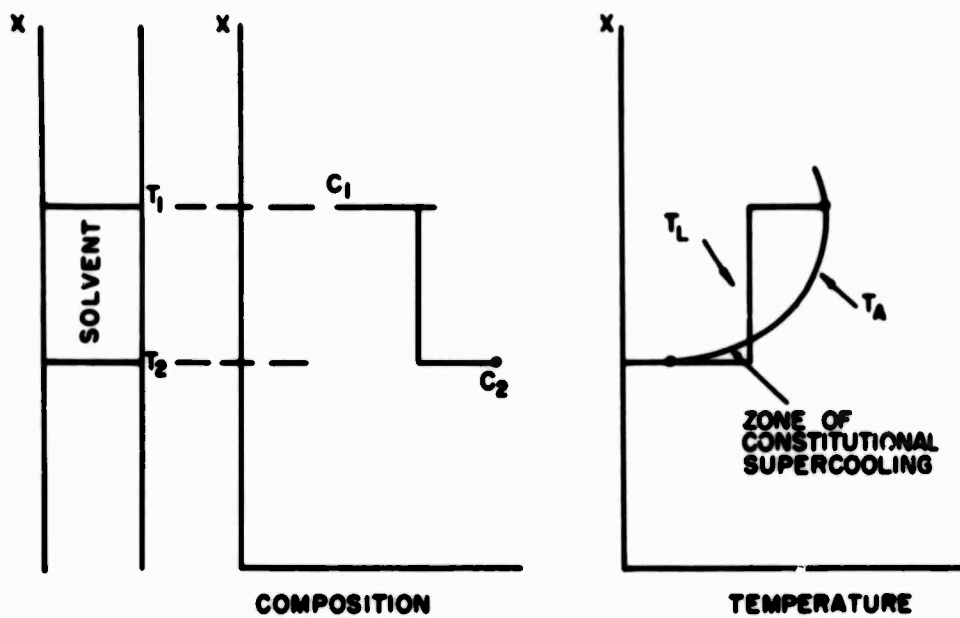


Fig. 5. Relation of concentration and temperature for the case of a fully stirred liquid

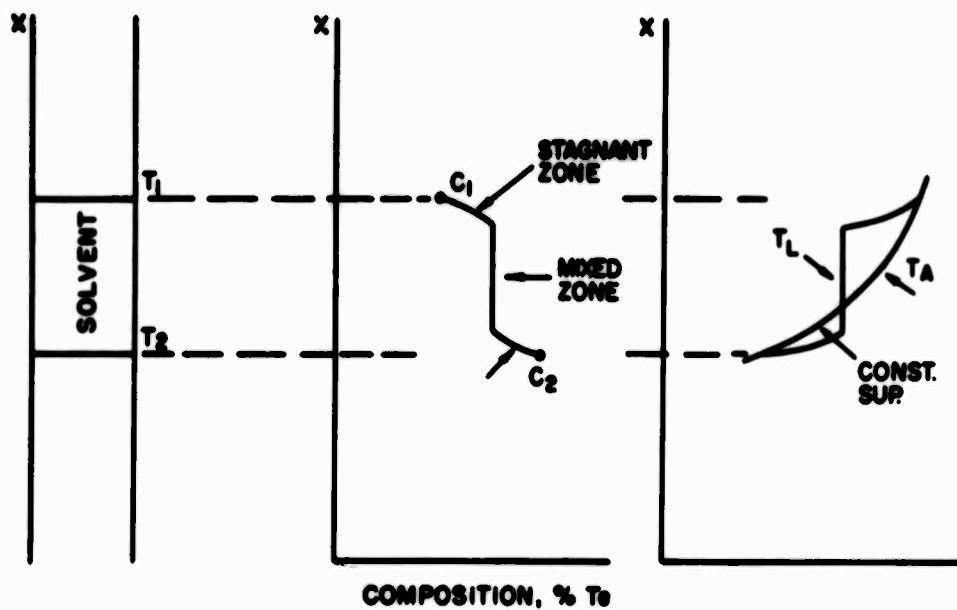


Fig. 6. Temperature and concentration distribution for the case of a partially stirred liquid

and  $T_2'$ . The liquid close to the interfaces will begin to change towards  $C_1'$  and  $C_2'$ ; after a short time, the composition profile would be curve B in Fig. 7; the liquidus temperatures will be shown on the left in Fig. 8. The actual temperature, however, will be as shown on the right; a supercooled region can exist near interface II if the temperature change is relatively fast. This effect is reduced by a steeper temperature gradient in the liquid, but this gradient is limited by the (usually high) thermal conductivity of the solvent.

### Interface Shape

The foregoing discussion suggests that, if the underlying assumption of planar interfaces is valid, substantial supercooling is unlikely but not impossible. However, the interface may not be planar. We will consider first the shapes of the isothermal surfaces that characterize the cases (a) when heat transfer from source to sink is by conduction alone, and (b) when there is sufficient mixing that the liquid is isothermal except in the two boundary layers, where heat transfer is by conduction. This will be followed by a discussion of the conditions under which the interface may deviate from the isotherm, and the possible consequences.

a. Heat transfer by conduction alone: In the (unrealistic) case in which the solid and the liquid have equal thermal conductivities, the thermal flow lines and the isotherms are shown in Fig. 9-a if the heat source is shorter (along the sample) than the heat sink, 9-b if the source is longer, and 9-c if they are equal. Cases b and c can be achieved in detail only by adding other flow lines; but the important feature of b, the existence of isotherms that are convex upwards, seems to be possible in a system like the one under consideration. It will be noted that Fig. 9-c includes the only case of a planar isotherm. It is not clear whether this is possible in the actual system, because the required symmetry requires isotherms such as AB, which implies another heat source lower down.

The assumption of equal thermal conductivities is unrealistic. In general the ratio is much larger than 1, which seems to mean that conditions close to Fig. 9-c would require the heat source to be four times as long as the heat sink. This suggests that conditions like 9-b can occur, and therefore that convex isotherms are possible; they are not under the conditions of Fig. 9-a, which, without the conductivity ratio, would be like the actual case.

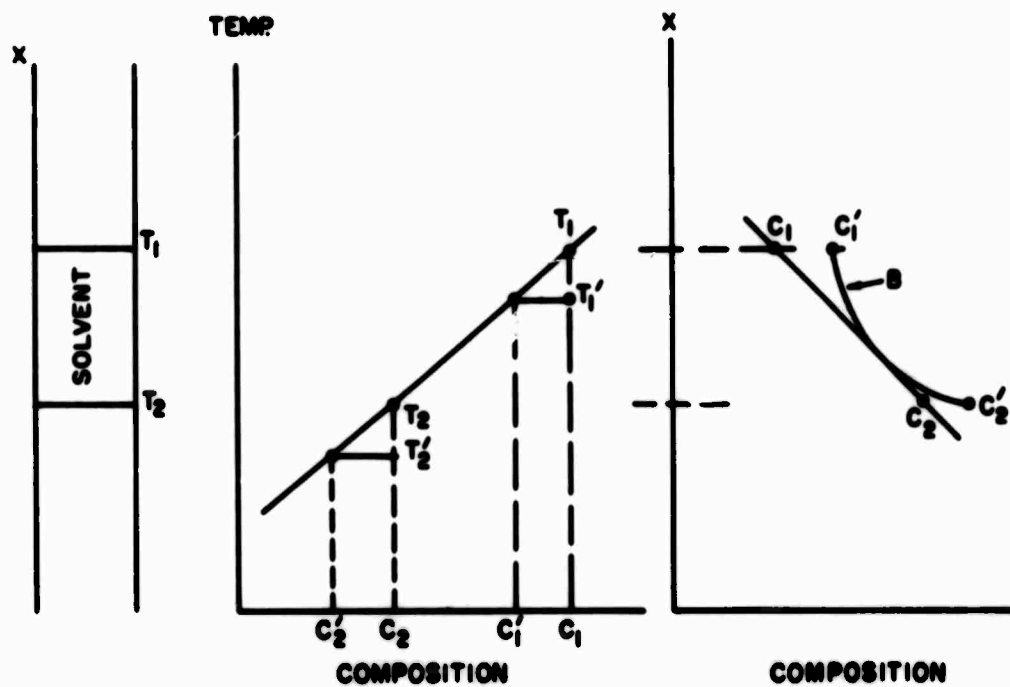


Fig. 7. Effect of temperature fluctuations on the concentration in a THM system

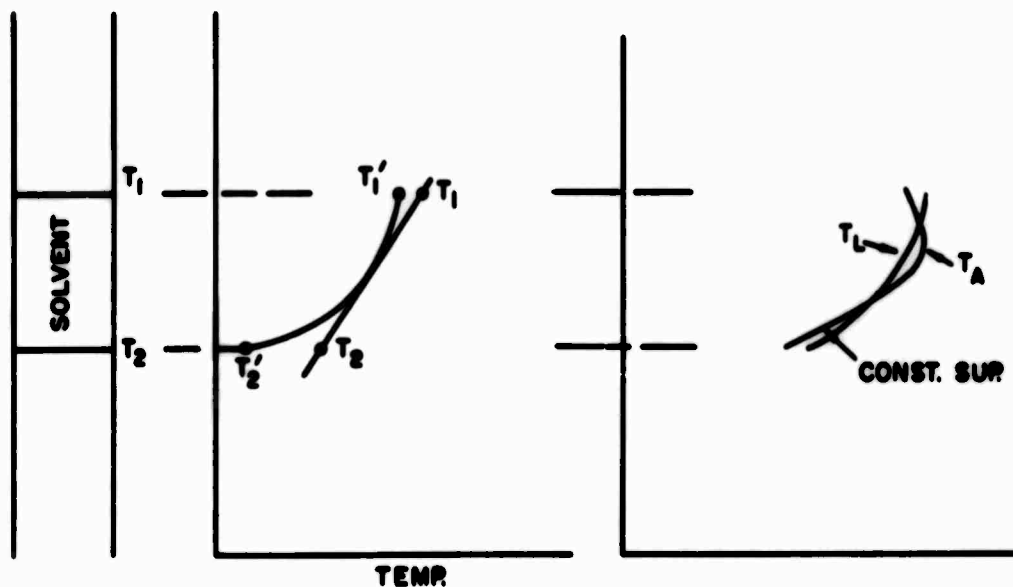
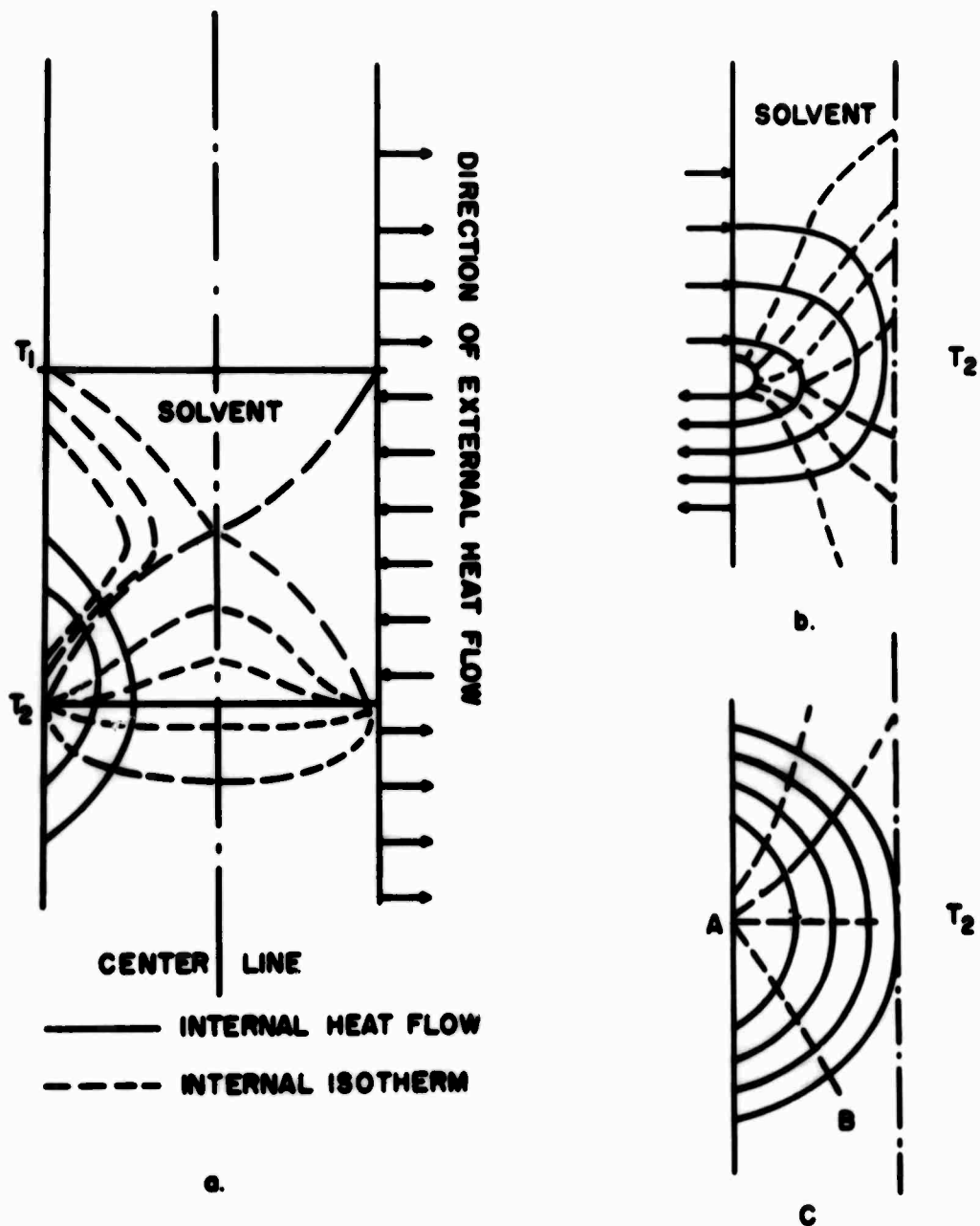


Fig. 8. Change of temperature profile in the solvent zone for the case of a sudden temperature drop



**Fig. 9.** Heat flow and isotherms in THM for the case of equal thermal conductivity in the solid and the liquid [(a) heat source is shorter than heat sink, (b) heat source is longer than heat sink, (c) heat source and sink are equal in length]

The volume of the liquid zone is essentially independent of the temperature distribution: it is bounded by isothermal surfaces at the liquidus temperatures for the composition of the liquid (this would be strictly correct for the static case when the zone is allowed to equilibrate, but not for the moving zone case). With any given temperature distribution (within a range that should be examined), there will always be two isotherms (equal or differing by the  $\Delta T$  required for the growth rate) that enclose the required volume of liquid. The problem is to adjust the temperature-liquid volume-speed relationship so that the isotherm at  $T_2$  has the optimum shape; in general, for a given temperature distribution, the greater the amount of liquid, the more concave the interface becomes (that is, lower interface concave to the liquid). Also, for a given amount of liquid, the lower the temperature, the more convex the interface becomes.

The ideal interface shape would be planar. This seems to be impossible, even ideally, because the system is not sufficiently symmetrical. The most undesirable situation seems to be a convex interface, because the perimeter would be starved of cadmium, lower its liquidus temperature, and drop below the  $T_1$  isotherm. Once this starts, the instability would develop further, eventually reaching (and probably overshooting) the eutectic point and then forming the tellurium rich phase. The local drop in interface temperature could also lead to constitutional supercooling and nucleation of new crystals.

The concave interface is less dangerous, because there is less cooling at the center than at the periphery. But if the density of the liquid increases with its tellurium concentration, then a pool of tellurium rich liquid would tend to form (by drainage) in the center, which could again cause a progressive drop in liquidus, possibly resulting in second phase and the nucleation of new crystals. The implication is that the interface should be maintained slightly but not drastically concave.

b. Interface shape, partially mixed liquid: Assume that the liquid is stirred sufficiently for all of it (except the two boundary layers) to be at the same temperature. The heat flow situation is now as shown in Fig. 10. It would seem that the interface isotherm could be planar or concave but not convex (convex would imply that heat is extracted more efficiently from the center than from the outer parts, as heat is, in this case, supplied uniformly everywhere). A slightly concave interface might be satisfactory, although the inherent disadvantages mentioned above might apply. The catastrophic instability near the surface would, however, be avoided.

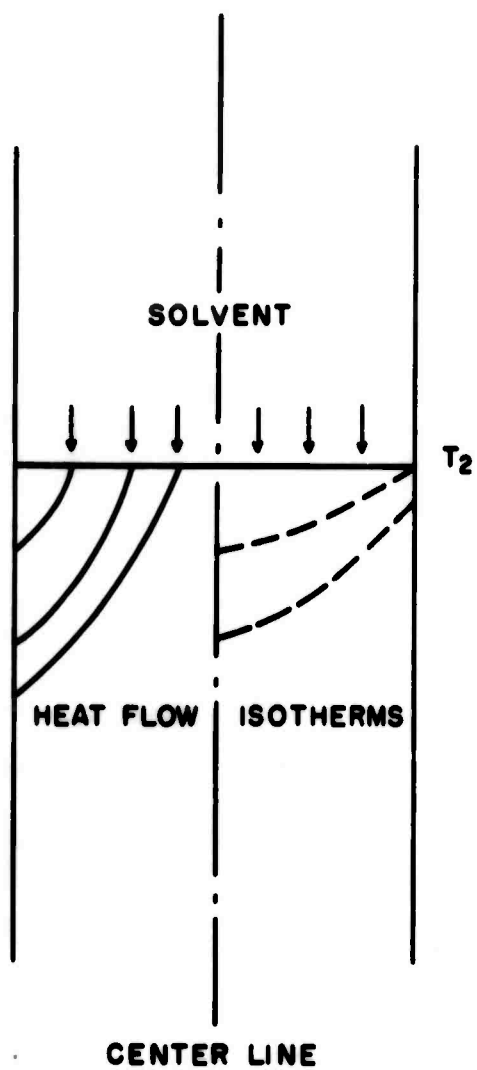


**Fig. 10.** Heat flow and isotherms in a partially mixed liquid

#### **4. Conclusions**

The major conclusions from the present analysis of the process would be that firstly the temperature gradient in the solvent (unless it became very small) would prevent constitutional supercooling at the growth interface. The only other condition leading to constitutional supercooling would be severe temperature fluctuations over the short term. Thus, good short term temperature control is essential and may lead to the necessity of controlling the voltage input into the furnace control system. This would avoid temperature changes due to fluctuations of voltage in the mains which can be severe enough and fast enough to override the control system. Secondly, some protection against at least short term power failures must be provided in any pilot production setup and developmental furnaces should at least possess some means of indicating short term power failures. But beyond this, the inevitable major conclusion is that the problems of inclusions and polycrystallinity may be attributed to unsatisfactory interface shape; because the temperature distribution is necessarily unsymmetrical, it may not be possible to achieve the optimum shape for both interfaces; the lower one is, however, much more critical, although severe departure of the upper one from a planar form would have some effect on the solute gradient. There is, however, no instability in the shape of the upper one. The analysis suggests that, if the interface profile can be observed and controlled (by sufficiently close temperature control), the unstirred liquid would be preferable, with a slightly concave interface. Since it seems not possible to do this, due to the fact that the solvent zone is stirred by the temperature gradient imposed on it, a minimally convex interface would be desirable.

#### **B. Crystal Growth\***

##### **1. THM-Experiments on the growth of cinnabar**

The foregoing discussion, then, highlights the fundamental problem of growing  $\alpha$ -HgS by the THM method. Due to the relatively low temperature at which cinnabar transforms to metacinnabar, a limitation on the growth temperature exists; the temperature at the growth interface must not exceed the transformation temperature of 344 °C. At these low temperatures, it becomes quite difficult to properly control the thermal conditions in order to maximize the temperature gradient into the

---

\*A.A. Menna and F. Wald

liquid, which avoids constitutional supercooling and stabilizes the growth process. Furthermore, it is equally difficult to achieve a sharp temperature drop at the growth interface in order to cause the required flat isotherm there.

Thus, it becomes extremely important to design a furnace which allows these thermal parameters to be optimized. Such a furnace design, which is now used in all growth experiments, is shown in Fig. 11. The furnace contains an insert of pyrolytic graphite with the crystallographic directions aligned such that radial heat flow is facilitated and longitudinal heat flow vastly decreased. Pyrographite, as used here, possesses a thermal conductivity of 3.9 which is better than that of copper in the radial direction and a thermal conductivity of 0.035 which is worse than that of alumina ceramic in the longitudinal direction. This combination of properties allows the highest possible temperature gradient in the liquid in conjunction with the highest possible drop at the liquid solid interface. The furnace profile is shown in Fig. 12, and a summary of all crystal growth runs for the last 6 months of the contract is found in Table III.

The various heat flow difficulties are compounded by the fact that an ideal solvent has not been found yet, although we find that  $K_2S_4$  which we presently use gives better results than  $Na_2S_4$  which is described in the literature.<sup>8</sup> Nevertheless, we believe that these polysulfides probably possess quite high viscosities, which limit the convection in the THM system, coupled with probably small diffusion coefficients for Hg, both of these properties hampering effective transfer of mercury for growth.

With these provisos in mind, we can now examine Table I which describes the crystal growth runs during the reporting period. It can readily be seen that the use of  $K_2S_4$  as a solvent at the highest possible interface temperatures was the most promising. In several cases, bright red transparent boules regrew, which contained fat needlelike crystals of  $\sim 1-2$  mm in diameter and 3-4 mm length (Fig. 13).

No evaluation other than optical transmission through the whole slice was performed on these ingots, but such measurements must be treated with caution since the boule did contain solvent inclusions.

Dr. A.N. Mariano of Kennecott Copper Corporation's Ledgemont Laboratories was kind enough to evaluate the growth habits of some of these crystals. His conclusions were that in some of the cases the habit of the crystals grown was purely rhombohedral with the only form present being  $\{10\bar{1}1\}$ . In other cases of solution grown crystals, well developed forms of both  $\{10\bar{1}1\}$  and  $\{01\bar{1}1\}$  were found.

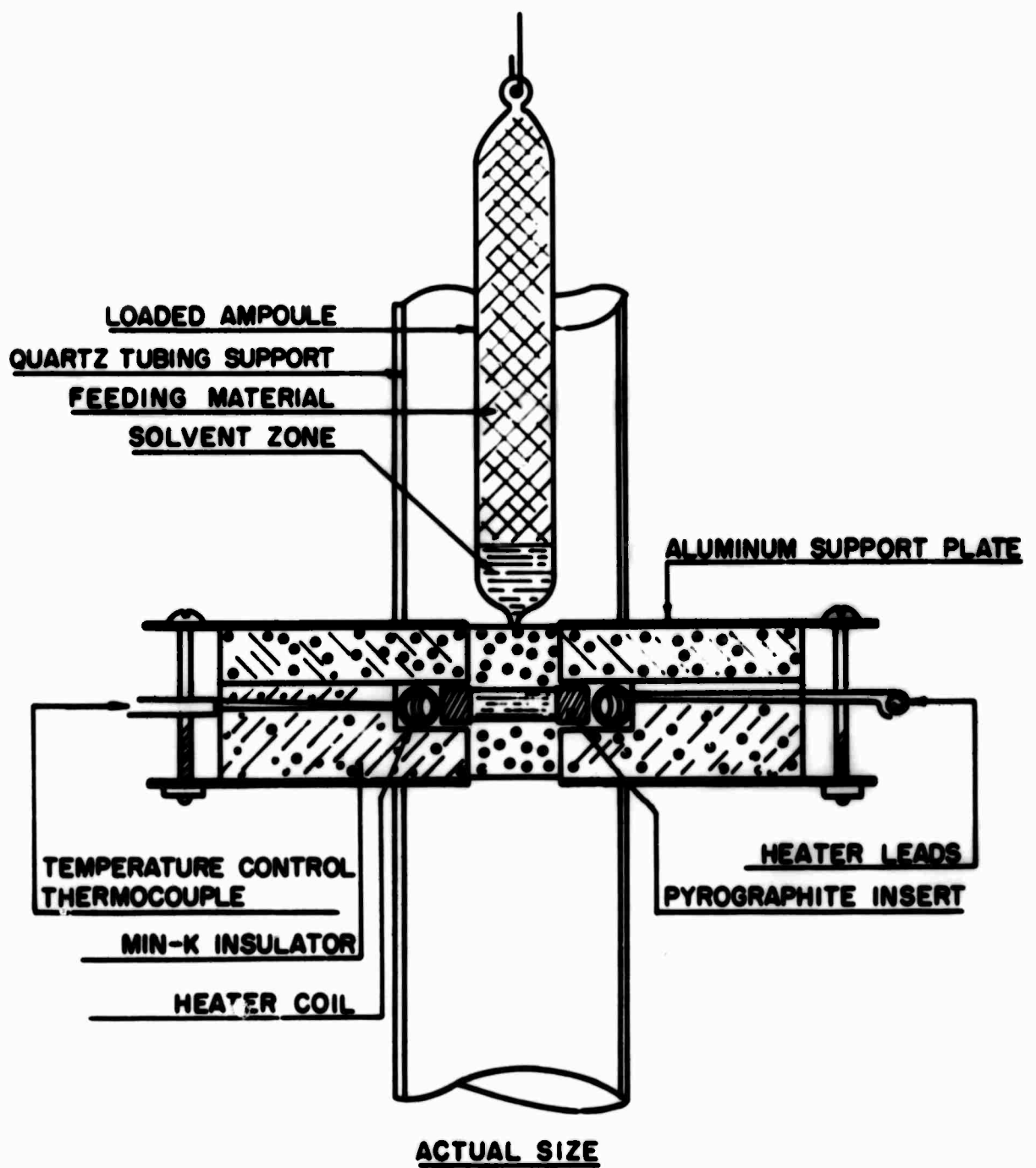
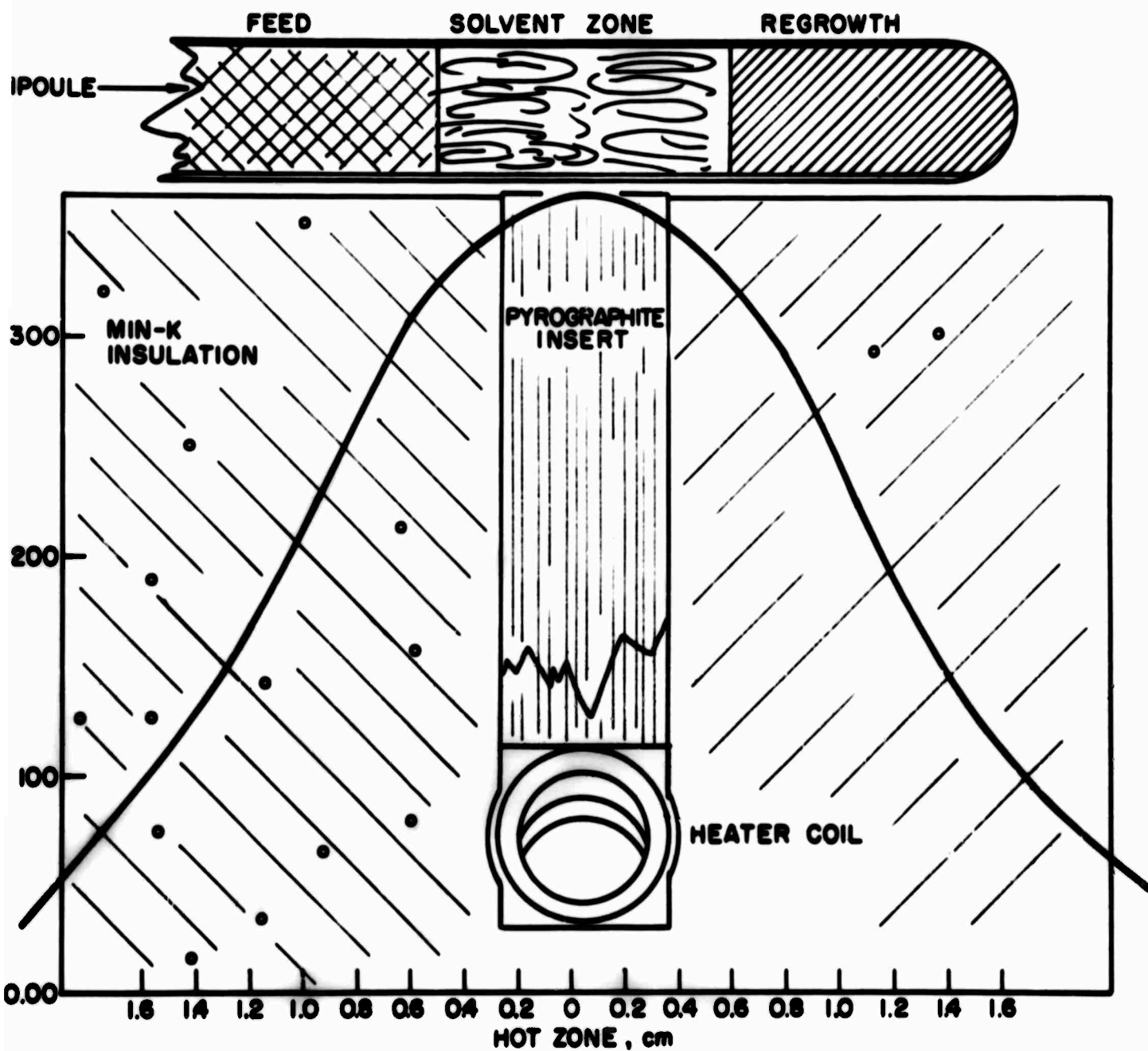


Fig. 11. Design of present THM furnaces



**Fig. 12.** Typical temperature profile in a TBM furnace as shown in Fig. 11



**Fig. 13. Cinnabar, regrown from  $K_2S_4$  in a THM experiment**

Table III. Crystal Growth Runs During the Last Months of the Contract

Run No.	Feed Material	Solvent Material	~ Zone Length	Temperature, °C	Drop Rate, mm/day	Comments
39	HgS, ~ 3.5-cm-long pellets	$\text{Na}_2\text{S}_4$	1 cm	310	3	Solvent didn't move, some vapor transport growth above solvent zone, { X-ray confirmed $\alpha$ -HgS crystals
40	$\text{Ag}_3\text{AsS}_3$ proustite, 6 cm long	$\text{Ag}_{1.4}\text{As}_{0.6}\text{S}_{1.6}$	1 cm	470		Regrown completely; some voids on outer surface
41	HgS, ~ 3.5-cm-long pellets	$\text{K}_2\text{S}_4$	1.2 cm	310		Elongated crystals above solvent zone, probably vapor transported regrowth
42	HgS packed powder, 3 cm	$\text{Na}_2\text{S}_3$ (cas.)	1 cm	310		Found some free sulfur plus some regrowth; not too impressive
43	HgS packed powder, ~ 3 cm	2.5 g Se + 0.359 g HgS	1 cm	310	3	Appears Se reacts to form HgSe + S, doesn't look promising
44	HgS, two-pellets, ~ 1.2 cm long	$\text{K}_2\text{S}_4$	0.5 cm	200	2.7	New heater, 0.5-cm zone, ~ 500 mm Ar pressure, very poly, regrowth used for run no. 48
45	HgS pellets, 3 cm long	$\text{Na}_2\text{S}_3$	0.5 cm	200	3	Very poly, many inclusions, ~ 500 mm Ar pressure, used for regrowth for run no. 48
46	Synthesis of proustite	—	—	600	Slow cooling	Cooled slowly; feed material for THM
47	Proustite, $\text{Ag}_3\text{AsS}_3$	$\text{Ag}_{1.4}\text{As}_{0.6}\text{S}_{1.6}$	1 cm	470	3	Ingot not too good, cracked, upper section transparent
48	HgS sections at no. 44-45	$\text{Na}_2\text{S}_4$	1.4 cm	334		Long needle-like crystals of $\alpha$ -HgS; many solvent inclusions
49	HgS from run no. 9, 2.8 cm	$\text{As}_2\text{S}_4$	11 mm	337		Formed a solid plug, transmission measurements of top slice
50	HgS, 3 cm of pellets	$\text{K}_2\text{S}_4$	1 cm	331		Two-zone furnace, upper ~ 200° C to prevent solvent creep, not impressive
51	Proustite from run no. 35, 4 cm cast	$\text{Ag}_{1.4}\text{As}_{0.6}\text{S}_{1.6}$	1 cm	460		Satisfactory; first to grow 2-cm unusually opaque, remainder transparent, somewhat poly
52	HgS (plug run no. 53), vapor grown	$\text{K}_2\text{S}_4$	1 cm	320		Polycrystalline elongated cluster, but zone didn't move very far
53	HgS powder	—	—	615 - 700	7	Grown solid plug for feed, very poly, used for run no. 52
54	HgS powder	—	—	615 - 700	7	Grown solid plug for feed, very poly, used for run no. 55
55	HgS vapor	$\text{As}_2\text{S}_3$	1 cm	338	3	Solvent zone didn't move
56	HgS vapor growth	—	—	615 - 700	7	Grown 3-cm plug, cinnamon plus metacinnabar, very poly, used for feed THM run no. 58
57	HgS vapor growth	—	—	615 - 700	7	2-cm plug, 8-mm diameter, last 2-3 mm appear quite bright red

Table III. (Cont.)

Run No.	Feed Material	Solvent Material	Approximate Zone Length	Temperature, °C	Prop. Rate mm/day
58	HgS plug run no. 58	$\text{Na}_2\text{S}_4$	1 cm	340	3
59	60 atom. % HgS 40 atom. % Hg <sub>2</sub> S	Hg <sub>2</sub> S	1 cm	310	3
60	HgS (run no. 53)	-	-	510-503	7
61	HgS powder	-	-	340	4
62	HgS powder	-	-	510	4.5
63	HgS powder	-	-	530-305	4.7
64	HgS plugs	$\text{K}_2\text{S}_4$	1 cm	334	5
65	Hg + S	-	~35 gm	Room temperature to 450	-
66	HgS 2 cm long, run no. 63	$\text{H}_2\text{S}_4$	1.2 cm	250	3
67	HgS powder	Vapor growth	-	630° hot end	~5
68	HgS pellets	$\text{K}_2\text{S}_4$	1 cm	200	~3
69	HgS powder	Vapor growth	-	615	-
70	HgS powder	Vapor growth	-	615	4
71	Bi + S ( $\text{Bi}_2\text{S}_3$ )	Synthesis and THM (Bi)	-	Room temperature - 750° slowly	-
72	HgS plug run 68	$\text{K}_2\text{S}_4$	~1 cm	200 °C	~3
73	HgS powder	Vapor growth	-	615	4
74	-	-	-	-	-

1 cm regrew very polycrystalline; 300 mm pressure Argon atmosphere

Regrew  $\text{Hg}_2\text{S}_3$  polycrystal in pot

Some small clear red crystals vapor growth

350 mm of Ar pressure; no regrowth; vapor growth

Plug grew in long needle like bundle with some faceted surfaces

Jet nozzle separated feed and regrowth chamber; fairly clean needle shaped crystals with distinct planes ~5 mm long regrew photo

Used 3 zone furnace to keep feed and solvent zone at approximately same temperature; appears as though solvent vapor grew  $\text{Hg}_2\text{S}$  - polycrystalline

Attempt to synthesize HgS from elements with excess sulfur, vapor pressure became too high - ampoule fractured at ~450 °C

Some regrowth with many solvent inclusions

Water cooled regrowth end of quartz cell - some transparent areas regrew near end of run

Some regrowth but temperature too low

Water cooled copper jacket used to cool growth end of ampoule plug grew but mixed mitacinnabar and cinnabar

Repeat of run 67 reduced quartz partition to 4mm thick between growth surface and cooling water produced mixed polycrystal boule

$\text{Hg}_2\text{S}_3$  made and THM with Bi - large 3-4 grains, no transmission band edge, ~1.2 eV; sulfur annealed at 500 °C made some grains IR transparent

Solvent did not move, no regrowth

Repeat of no. 70 except quartz partition 1 cm long between water and growth

Surface large grained plug - some red to dark red; no transmission

Table III. (Cont.)

Run No.	Feed Material	Solvent Material	Approximate Zone Length	Temperature, °C	Proposed Rate, mm/day	Comments
75	Bi <sub>2</sub> S <sub>3</sub> syntheids	Bridgman grown	-	770	5	Very clean bright ingot - slice anneal ~3 days in sulfur at 530, no transmission; carrier concentration ~10 <sup>13</sup>
76	HgS ~2 cm run no. 72	K <sub>2</sub> S <sub>4</sub>	1 cm	504	2.3	Indications showed the need for higher zone temperature, the zone appears to have passed completely through the feed; photos
77	HgS powder and plug	Hydrothermal growth, 0.5M Na <sub>2</sub> S solution	-	240	-	Third day heater control failed, rupture disk blew, lost contents
78	HgS powder	Vapor growth	-	~700	2	Solid plug formed, polycrystalline; good interface
79	HgS packed powder	K <sub>2</sub> S <sub>4</sub>	1.7	450 and 1/3 atmosphere Argon	3	Densely packed plug regrew, ~2% transmission; some solvent inclusions, looks promising
80	HgS plug for run no. 73	K <sub>2</sub> S <sub>4</sub>	1 cm	~500 in vacuum	2.3	Solid plug regrew, some solvent inclusions - red
81	HgS powder	Vapor growth	-	~527 in vacuum	5	Good plug for THM regrowth
82	Bi <sub>2</sub> S <sub>3</sub> (run no. 75)	Bi	1 cm	600	5	Regrowth good 2-3 large grains at top; no transmission photos
83	HgS plugs (run 41)	K <sub>2</sub> S <sub>4</sub>	1.6 and 1/3 atmosphere Argon	530	3	In progress
84	HgS 10 g	K <sub>2</sub> S <sub>4</sub> 30 g	-	To 500	-	~30 hr at 500 °C than slow cooling ~10°/hr, formed microclinal cubic needles; saturated solvent will be used for THM growth
85	Bi <sub>2</sub> S <sub>3</sub> ingot from no. 82	Te	1	650	2.7	Solvent moved through feed, produced low resistivity material
86	HgS hydrothermal growth	0.5M solvent Na <sub>2</sub> S	-	~300° ~300 psi	-	Pressure dropped after ~3 days into run, had to shut down

## **2. Other methods of crystal growth applied to cinnabar**

a. **Vapor growth:** For the vapor growth, a modified Piper and Polich technique which had been used at Tyco before for the growth of CdS was used (Fig. 14). In it, the end of an ampoule is slowly withdrawn from a furnace such that a solid crystalline body grows from the tip of the ampoule, slowly filling the whole space. The process leads to growth of a solid plug of HgS, 3 cm long in about 4 days under the following conditions: hot side:  $\sim 600$  to  $700^{\circ}\text{C}$  and estimated growth temperature:  $\sim 300$ - $350^{\circ}\text{C}$ .

Fig. 15 shows an ingot prepared in this way, sectioned along its length. Under the microscope it can be seen that this ingot is in fact red colored and thus is most likely cinnabar. Although microscopically no evidence could be found that the plug had cooled through the metacinnabar/cinnabar transformation, we still have doubts whether all of the material grew initially as cinnabar. So far, irrespective of the temperature gradients used, only very polycrystalline ingots or collections of rods were grown (Fig. 16). Such rods or longer needles grown on the walls were also evaluated by Dr. Mariano as to their growth habits. Longer needles were found to be well formed prisms with  $\{10\bar{1}0\}$  habits twinned with  $\{0001\}$  as the composition plane. Other habits found in vapor growth experiments were short stubby crystals with well developed  $\{10\bar{1}1\}$  and  $\{01\bar{1}3\}$  forms.

b. **Hydrothermal growth:** Three experiments have been attempted using the hydrothermal growth method of crystal growth discussed by Y. Toudic and R. Aumont<sup>9</sup> and also S.D. Scott and H.L. Barnes.<sup>10</sup> The procedure used was as follows: The autoclave (made by Autoclave Engineers, Inc.,) was thoroughly cleaned and dried and the Teflon insert fitted with a seed holder at the bottom and  $2/3$  up from the bottom (see Fig. 17). The bottom seed was a slice of single crystal of CdS. The top was a Teflon cup which contained  $\sim 8$  g of vapor-grown polycrystalline HgS material. A fresh solution of  $0.5\text{M Na}_2\text{S}$  was prepared and  $\sim 1\text{l}$  was saturated with 25 g of HgS powder. The saturated solution was carefully poured into the Teflon container which fitted tightly with the autoclave so that very little space was left for condensate to collect. The top flange was bolted down firmly and the heating tape which surrounded the stainless steel vessel was turned on. Approximately 24 hr later the temperature stabilized  $\sim 230^{\circ}\text{C}$  and pressure of 406 psia. The use of Teflon as a container forbids any higher temperature.

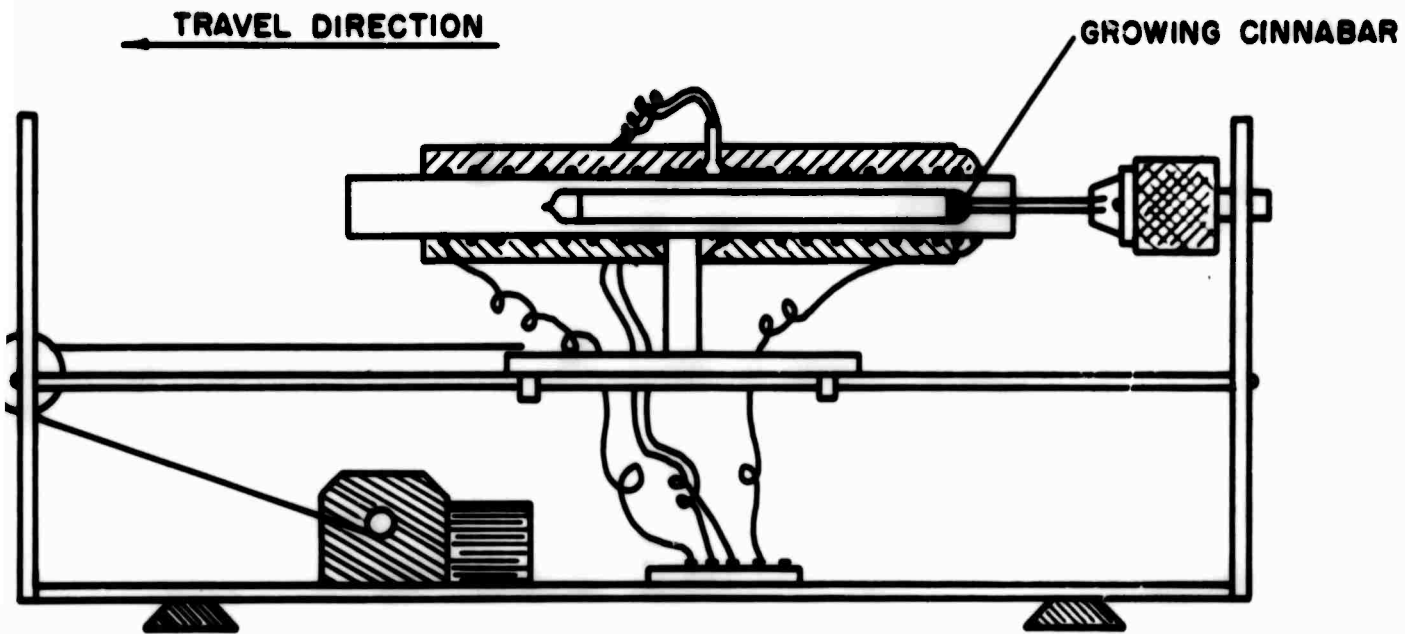
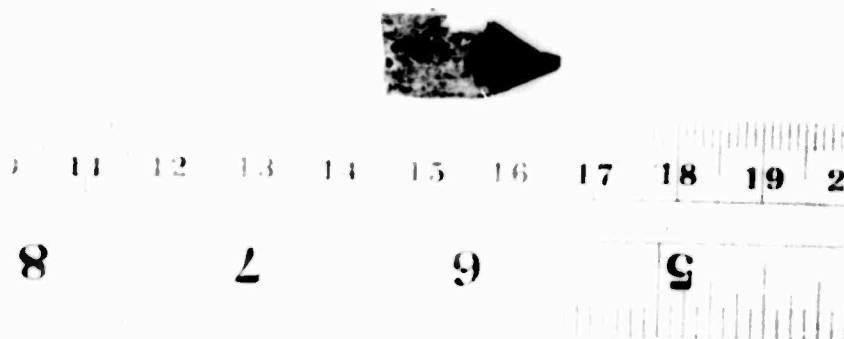
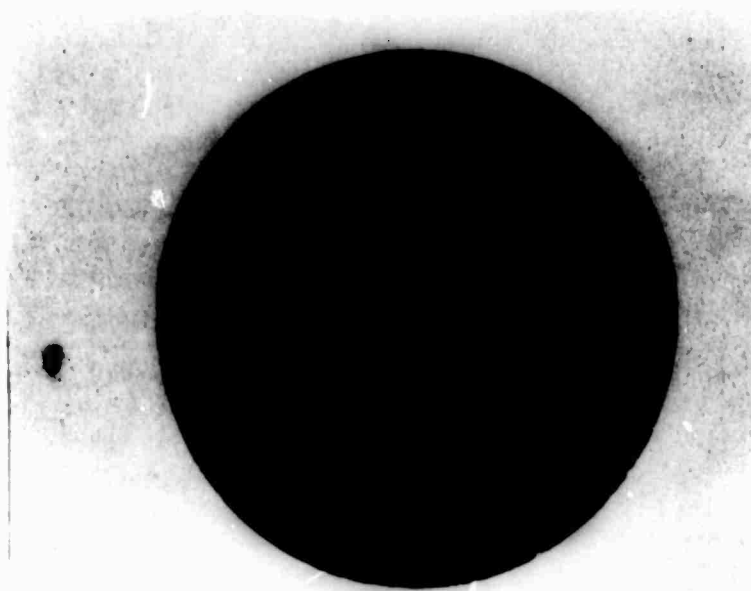


Fig. 14. Schematic of  $\alpha$ -HgS vapor growth furnace



**Fig. 15.** Longitudinal section through vapor grown polycrystalline  $\alpha$ -HgS boule



**Fig. 16.** Top of vapor grown  $\alpha$ -HgS ingot showing a series of rods

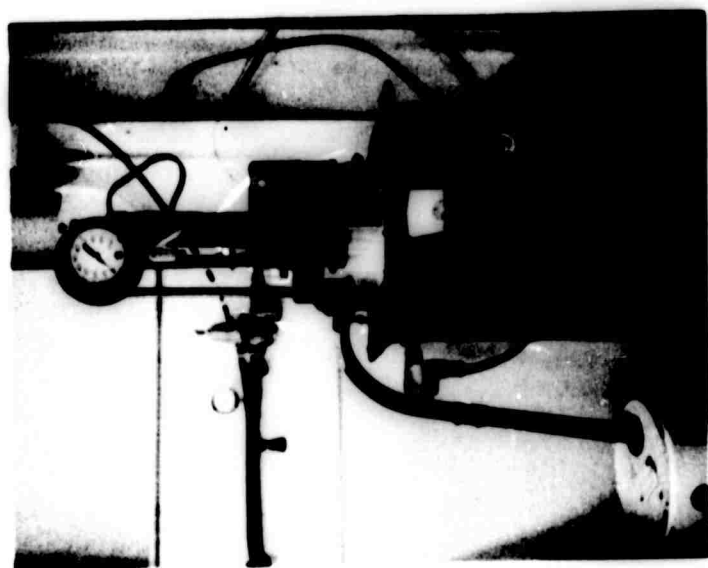
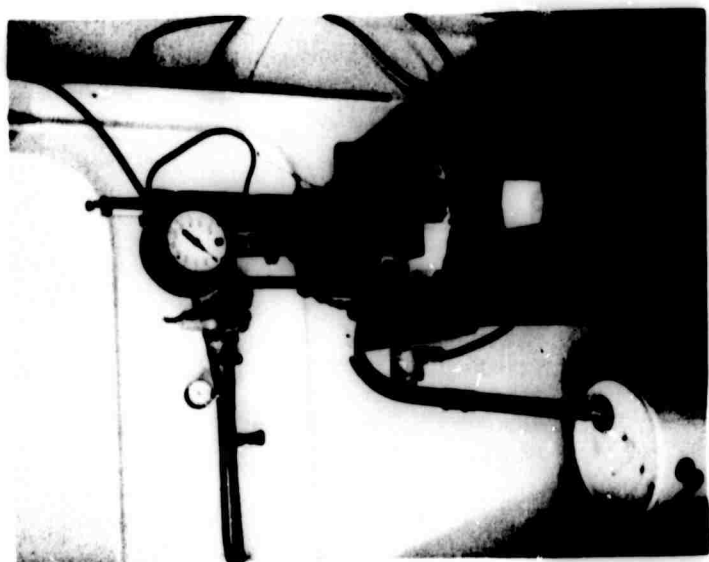


**Fig. 17. Autoclave used in hydrothermal growth experiments**

During the experiment, the solution is stirred slowly (~ 30 rpm) to aid the nutrient diffusion to the seed site. Results for the first two experiments have been negative due to the fact that the autoclave developed a leak after 3 or 4 days running and had to be shut down. In the third attempt, however, some indication that a CdS seed may work was obtained since some HgS did begin to grow on the substrate, despite a leak which eventually terminated the experiment.

### 3. Growth of materials other than cinnabar

Some experiments on the growth of  $\text{Bi}_2\text{S}_3$  were started. It has been variously reported that this compound has a band gap between 1.1 and 1.3 eV and can be made with a high resistance if excess sulfur is employed.<sup>11</sup> Thus, we felt that the high molecular weight coupled with a high bandgap and an asymmetrical structure might make the material worth looking at for electrooptic purposes. Thus  $\text{Bi}_2\text{S}_3$  ingots were grown by the Bridgman method and by THM from Bi and subsequently annealed in a sulfur atmosphere. Also, growth from Te was attempted with the aim of filling the S vacancies. So far, the results were disappointing, since no material of optical transparency and high resistivity was obtained.

Further experiments on the growth of proustite were also conducted with much the same results as in the first half of the contract which demonstrated that proustite can indeed be grown by THM. All these runs are also summarized in Table III.

#### IV. CONCLUSIONS

THM growth of  $\alpha$ -HgS has proven to be quite difficult although at present it is not definitely clear whether the method can succeed.

Vapor growth of the compound does not seem to be practicable for large crystals although it is an excellent means to provide solid boules of purified polycrystalline material for regrowth by THM.

Hydrothermal growth has shown some initial promise and will be pursued further. Also, some gel-growth experiments are planned.

$\text{PbCsCl}_2$  and by inference  $\text{PbCsBr}_3$  can be grown if needed by THM from  $\text{PbCl}_3$  ( $\text{PbBr}_2$ ) melts. Proustite can be grown from  $\text{As}_2\text{S}_3$  rich compositions in the  $\text{Ag}_2\text{S} - \text{As}_2\text{S}_3$  system. It is transparent and, with some minimal further work, could be obtainable in good quality. If indeed the fact of the disappearance of the  $10\text{-}\mu$  absorption peak in such solution grown material can be confirmed, THM might provide better quality material.

$\text{Bi}_2\text{S}_3$  can be grown by THM from Bi solvents. It is obtained with good crystalline quality in this case. Nevertheless, it possesses high carrier concentrations and therefore high IR absorption. Other solvents such as Te or annealing procedures have not yet effected any significant change.

## **V. REFERENCES**

- 1. G. A. Wolff and H. E. LaBelle, J. Amer. Cer. Soc., 48, 441 (1965).**
- 2. B. diBenedetto and C. J. Cronan, J. Amer. Cer. Soc., 51, 364 (1968).**
- 3. R. O. Bell, N. Hemmat and F. Wald, Physica Stat. Sol.(a) 1, 375 (1970).**
- 4. Fritz V. Wald, Richard O. Bell, and Andrew A. Menna, Electrooptic Modulator, Tyco Laboratories for Air Force Cambridge Research Laboratory, sponsored by Advanced Research Projects Agency, First Quarterly Report, Sept. 1970 and Semiannual Report No. 1., Jan. 1971.**
- 5. R. O. Bell and G. Rupprecht, Phys. Rev., 123, 97 (1961).**
- 6. I. P. Kaminow and E. H. Turner, Proc. IEEE, 54, 1374 (1966).**
- 7. G. E. Peterson, P. M. Bridenbaugh and P. Green, J. Chem. Phys., 46, 4009 (1967).**
- 8. R. W. Garner and W. B. White, J. Crystal Growth, 7, 343 (1970).**
- 9. Y. Taudic and R. Aumont, Laboratory, C.N.E.T.-C.N.R.S.-C.N.E.T., Route Tregastel 22, Lannion France; presented at the Third International Conference of Crystal Growth, Marseille, France, July 1971.**
- 10. S. D. Scott and H. L. Barnes, Dept. of Geochemistry and Mineralogy, The Pennsylvania State University, University Park, Pennsylvania 16802.**
- 11. N. Kh. Nriksosov, et al., Semiconducting II-VI, IV-VI and V-VI Compounds; Plenun Press, New York 1969, pp. 167-168, p. 190.**